MOLECULAR IMAGING AND BIOLOGY

Mol Imaging Biol (2017) 19:656–664
DOI: 10.1007/s11307-016-1041-y

Published Online: 17 February 2017

RESEARCH ARTICLE

Molecular Simulation of Receptor Occupancy and Tumor Penetration of an Antibody and Smaller Scaffolds: Application to Molecular Imaging

Kelly D. Orcutt,[1] Gregory P. Adams,[2,3] Anna M. Wu,[4] Matthew D. Silva,[1] Catey Harwell,[1] Jack Hoppin,[1] Manabu Matsumura,[5] Masakatsu Kotsuma,[5] Jonathan Greenberg,[6] Andrew M. Scott,[7,8,9] Robert A. Beckman[10,11,12,13]

[1]*inviCRO, LLC Boston, 27 Drydock Ave., 7th Floor West, Boston, MA, 02210, USA*
[2]*Developmental Therapeutics Program, Fox Chase Cancer Center, Philadelphia, PA, USA*
[3]*Viventia Bio, 3711 Market Street, Philadelphia, PA, 19104, USA*
[4]*Department of Molecular and Medical Pharmacology, David Geffen School of Medicine at UCLA, Los Angeles, CA, USA*
[5]*RD Division of Daiichi Sankyo Co., Ltd., Tokyo, Japan*
[6]*Daiichi Sankyo Pharmaceutical Development, Edison, NJ, USA*
[7]*Olivia Newton-John Cancer Research Institute, Melbourne, Australia*
[8]*Department of Molecular Imaging and Therapy, Austin Hospital, Melbourne, Australia*
[9]*La Trobe University, Melbourne, Australia*
[10]*Department of Oncology, Georgetown University Medical Center, Washington, DC, USA*
[11]*Department of Biostatistics, Bioinformatics, and Biomathematics, Georgetown University Medical Center, Washington, DC, USA*
[12]*Lombardi Comprehensive Cancer Center, Georgetown University Medical Center, Washington, DC, USA*
[13]*Innovation Center for Biomedical Informatics, Georgetown University Medical Center, Washington, DC, USA*

Abstract

Purpose: Competitive radiolabeled antibody imaging can determine the unlabeled intact antibody dose that fully blocks target binding but may be confounded by heterogeneous tumor penetration. We evaluated the hypothesis that smaller radiolabeled constructs can be used to more accurately evaluate tumor expressed receptors.

Procedures: The Krogh cylinder distributed model, including bivalent binding and variable intervessel distances, simulated distribution of smaller constructs in the presence of increasing doses of labeled antibody forms.

Results: Smaller constructs <25 kDa accessed binding sites more uniformly at large distances from blood vessels compared with larger constructs and intact antibody. These observations were consistent for different affinity and internalization characteristics of constructs. As predicted, a higher dose of unlabeled intact antibody was required to block binding to these distant receptor sites.

Electronic supplementary material The online version of this article (doi:10.1007/s11307-016-1041-y) contains supplementary material, which is available to authorized users.

Correspondence to: Kelly Orcutt; *e-mail:* orcutt@invicro.com

Conclusions: Small radiolabeled constructs provide more accurate information on total receptor expression in tumors and reveal the need for higher antibody doses for target receptor blockade.

Key words: Receptor occupancy, Tumor penetration, Antibody imaging, Antibody scaffolds, Mathematical model, Tumor antigen

Introduction

Optimal dosing of monoclonal antibodies should allow sufficient exposure for uniform penetration of tumors, so that no tumor cells can escape therapy simply due to inhomogeneity of tumor penetration. Receptor occupancy should be sufficient, both in number and duration, for tumor cell kill [1].

In vivo imaging is a technique that can be used to non-invasively evaluate receptor occupancy in all lesions at once. In a traditional competition experiment (Fig. 1) [2], competition between labeled antibody and increasing mass dose of unlabeled antibody in successive cohorts of patients is used to infer the dosage required for receptor saturation. However, if the labeled and unlabeled antibodies do not penetrate uniformly, competition may occur only at accessible sites, while other relevant sites with living tumor cells may be inaccessible and thus not interrogated (Fig. 2) [2]. In an attempt to circumvent this issue, the "enhanced competition experiment (ECEX)," has been proposed, in which the labeled moiety is smaller and more diffusible, such that it can penetrate tumors more deeply and homogeneously (Fig. 3) [2]. The hypothesis is that a higher dose of unlabeled antibody may be required to penetrate deeply into tumors and fully displace a diffusible labeled smaller construct from less accessible sites [2]. We refer to this hypothesized phenomenon as the enhanced competition effect (ECE).

Here, a series of simulation studies were performed to explore traditional and enhanced competition from a theoretical standpoint and to answer the following questions: (1) Can the ECEX be simulated mathematically? (2) Is an increased dose of antibody required to achieve saturation in the ECEX, according to the ECE hypothesis? (3) What is the effect of tumor variables on the result (intervessel distance, receptor number, internalization kinetics, *etc.*)? (4) What are the properties of a small construct that would be needed to perform such an experiment (size, affinity, *etc.*)? and (5) Can this experiment be performed using current technology?.

The simulations utilized parameters derived from the literature [3–10] and the Krogh cylinder model [11–13], modified to take bivalent binding of constructs into account, and to consider a realistic distribution of variable intervessel distances [14]. Differential equations describing the transport and kinetics of both unlabeled and competing labeled construct were solved simultaneously. The

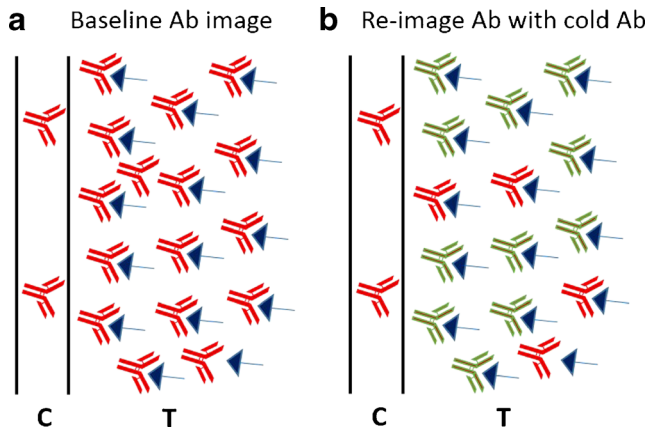

Fig. 1 The traditional competition experiment by imaging. *C* capillary, *T* tumor. The target antigen is represented by *blue arrows*. Labeled and unlabeled monoclonal antibodies are represented by *red* and *green antibody shapes*, respectively. **a** The first step is baseline imaging of radiolabeled monoclonal antibody. **b** After the radioactivity in the labeled dose has decayed, imaging of the radiolabeled antibody is repeated in the presence of unlabeled monoclonal antibody given concurrently in increasing mass doses to successive cohorts of patients. This blocks an increasing number of target antigen sites depending on the dose. From the mathematical form of the blockage as a function of dose, the dose that would give complete blockage is inferred.

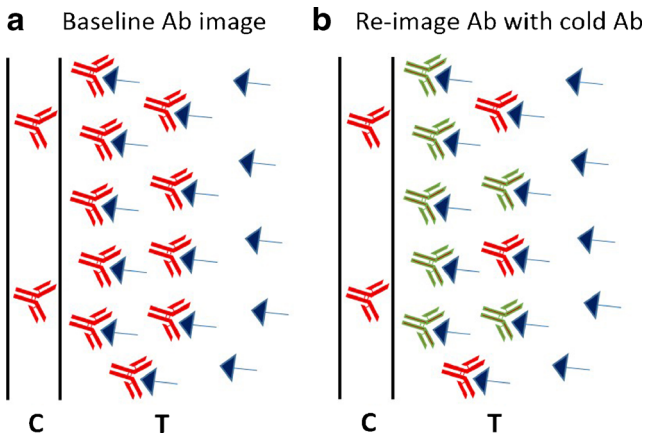

Fig. 2 The traditional competition experiment by imaging, potentially addressing only the most accessible sites in the tumor. *C* capillary, *T* tumor. The target antigen is represented by *blue arrows*. Labeled and unlabeled monoclonal antibodies are represented by red and green antibody shapes, respectively. The experiment may offer no information about doses needed to bind antigen deep within the tumor where neither the labeled or unlabeled antibody penetrate, and therefore there is no competition occurring. See legend to Fig. 1 for further explanation of (**a**) and (**b**).

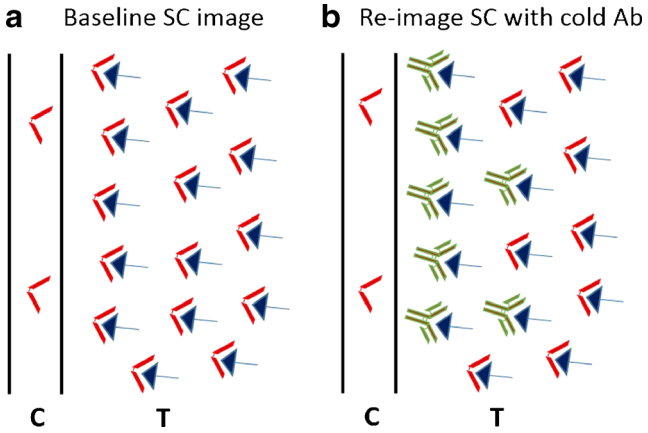

Fig. 3 The enhanced competition experiment. *C* capillary, *T* tumor. The target antigen is represented by *blue arrows*. Labeled small construct (SC) is represented by *red angles*. Unlabeled full-length monoclonal antibodies are represented by the *green antibody shapes*. **a** The first step is baseline imaging or radiolabeled SC. Compared with the radiolabeled, full-length monoclonal antibody in Fig. 2a, the labeled SC penetrates the tumor more thoroughly, including the target antigens deep within the tumor. **b** After the radiolabeled SC has been washed out from the tumor (more rapidly than with full-length monoclonal antibody), imaging of the radiolabeled SC is repeated in the presence of unlabeled monoclonal antibody given concurrently in increasing mass doses to successive cohorts of patients. This blocks an increasing number of target antigen sites depending on the dose. Compared with Fig. 2b, we see that binding of the SC deep within the tumor has revealed that the cold full-length monoclonal antibody did not block these less accessible sites, and higher dosages of full-length monoclonal antibody may potentially be required to block all the sites. From the mathematical form of the blockage as a function of dose, the dose that would give complete blockage is inferred.

concentrations of free, bound and internalized compounds were solved as a function of time and distance from the capillary wall. Three-dimensional surface plots were generated to display compound penetration into the tumor interstitial tissue over time.

Materials and Methods

Parameters Used for the Simulation

Four different parameter sets (antibody dissociation constant (K_D), antigen number/cell (B_{max} no./cell), and internalization half-life) representing antigen and antibody pairs were used for the mathematical simulations (Table 1). The parameter ranges are in accord with those reported in the literature as described below.

Table 1. Parameters used in mathematical simulations

	K_D (nM)	B_{max} no./cell	Internalization half-life
Ab1	0.1	18,000	5 min
Ab2	10	36,000	45 min
Ab3	1	60,000	75 min
Ab4	3	150,000	13 h

Ab1–Ab4 are virtual antibodies created using parameters from the literature

Antibody Dissociation Constant

Thurber and Wittrup [3] reported the value as 10^{-12}–10^{-6} M (1–10 nM, in general for IgGs). Thus, K_D was varied from 0.1 to 10 nM (monovalent affinity).

Antigen Number/Cell

There are several reports on EGFR (the target for cetuximab) [4] and CD20 (the target for rituximab, ofatumumab, and obinutuzumab) [5, 6] expression number in cell lines and human samples. The expression number is variable but typically ranges between 10^4 and 10^5 copies/cell.

Internalization Half-Life

HER2 (the target for trastuzumab) internalization rate (k_e) is reported from 1.6×10^{-3} to 1.6×10^{-4} s^{-1}, corresponding to ca. 7 to 70 min as internalization half-lives [7, 8]. The internalization half-life of CD20 measured by rituximab, ofatumumab, and obinutuzumab is reported between 30 and 7 h [9]. In a study in which internalization of ^{64}Cu-DOTA-cetuximab was evaluated in EGFR-positive cell lines, internalization was linear for the first 15–30 min but began to plateau after approximately 1 h [10]. These results suggest internalization half-lives of clinically applicable antibodies are on the order of minutes to hours. Thus, a broad range from 5 min to 13 h was selected for the internalization half-life in this simulation study.

Distributed Krogh Cylinder Simulations

Numerical simulations were carried out for both traditional and enhanced competition using Krogh cylinder geometry [11] (Fig. 4).

The published Krogh cylinder model [11–13] was modified to incorporate bivalent binding into the equations using the effective concentration of the second binding site to determine the increase in avidity for bivalent compounds. The differential equations, boundary conditions, and initial conditions used in the simulations are defined in the Electronic Supplemental Materials.

Blood pharmacokinetic parameters for each compound are given in Table 2 and are derived from literature

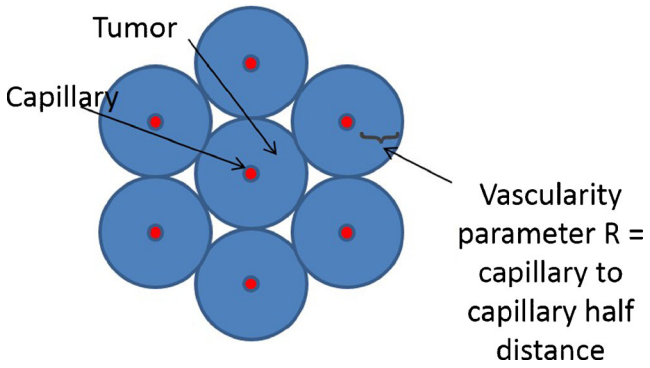

Fig. 4 Schematic of Krogh cylinder geometry with cylindrical tumor capillaries surrounded by cylindrical tumor interstitial tissue. The Krogh radius *R* is the capillary to capillary half-distance.

experimental concentration data in %ID/ml units following a bolus intravenous administration of the compound in mice. Data points were fit to a bi-exponential model where A is the fraction of alpha phase clearance, $t_{1/2,\ alpha}$ is the alpha phase half-life and $t_{1/2,\ beta}$ is the beta phase half-life [15–28].

The beta phase half-life for the affibody is notably longer than the other smaller molecular weight scaffolds and appears to be due to a small amount of material that remains in the blood for an extended period of time [17, 18].

To simulate tumors with a distribution of vessel distances, the results from Krogh cylinder model simulations were weighted with the following weighting factors (R = 50 μm, 0.05; R = 100 μm, 0.2; R = 150 μm, 0.7; and R = 300 μm, 0.05) informed from Lauk *et al.* [14]. For sub-saturating antibody doses, the penetration distance is smaller than the Krogh cylinder radius and the antibody does not interact with the outer Krogh cylinder boundary. However, as saturation is approached, the antibody reaches the Krogh cylinder boundary and this is conceptually when the vessel distance terms start to interact. It is important to include varying radii to most accurately represent the *in vivo* scenario especially when considering doses that span sub-saturating to saturating levels. All simulations reported herein assumed simultaneous injection of labeled and unlabeled constructs.

Results

Traditional competition simulations showed that unlabeled antibody competes with radiolabeled antibody only for binding sites close to the capillary wall (Fig. 5a, arrows) under conditions of sub-saturation. In an analogous simulation with all parameters equal except for the radiolabeled construct molecular weight (and parameters impacted by molecular weight), a 2-kDa peptide shows significantly increased penetration away from the capillary compared with the unlabeled antibody (Fig. 5b, arrows). These results demonstrate that the ECEX can be mathematically simulated. Plots showing the separate free, monovalently bound, bivalently bound, and internalized compound species for the results presented in Fig. 5 are shown in Supplementary Fig. S1.

Table 2. Molecular weight and blood pharmacokinetic parameters for each construct

Parameter	Antibody	Minibody	Diabody	scFv	Affibody	Peptide
MW (kDa)	150	80	50	25	7	2
A	0.47	0.4	0.94	0.8	0.998	0.998
$t_{1/2,\ alpha}$ (h)	7.3	0.657	0.37	0.05	0.244	0.138
$t_{1/2,\ beta}$ (h)	271	5.23	7.1	3	23.1	5

Mathematical simulations of ECEXs were performed for multiple "small constructs" including 80 kDa minibody, 50 kDa diabody, 25 kDa scFv, 7 kDa affibody, and 2 kDa peptide constructs to investigate the effect of molecular weight on tumor penetration and ECE (Supplementary Fig. S2). These simulations suggest that a molecular weight of 25 kDa or below is required for sufficient tumor penetration for enhanced competition.

In an attempt to (1) observe the effect of an increased dose of unlabeled antibody on imaging signal at one time point and (2) compare different molecular weight constructs, the optimal imaging time for each construct was defined as the time at which the tumor signal minus the blood signal was maximal. Using this optimal imaging time point for each construct, a single plot with the traditional dose escalation experiment and ECEXs with the different sized constructs was constructed (Fig. 6, Ab1 and Ab3; Supplementary Fig. S3, Ab2 and Ab4). An increased dose of antibody is required to achieve saturation in the ECEX for the affibody and 2 kDa peptide for Ab1, Ab2, Ab3, and Ab4, documenting the ECE for these four different virtual antibodies. Results shown are with a 1-μg (0.04 mg/kg) dose of radiolabeled construct. Similar results were observed for 10 μg (0.4 mg/kg) and 100 μg (4 mg/kg) (data not shown). The magnitude of the ECE is defined as the ratio of the unlabeled antibody dose required for 99 % saturation by the ECEX and the unlabeled antibody dose required for 99 % saturation by traditional competition. The ECE magnitude may be compared for the four different virtual antibodies by comparing the saturation points for the labeled antibody versus labeled peptide in Fig. 6b, d and Supplementary Fig. S3 (arrows) and ranges between approximately 2- and 10-fold for the antibody parameters studied here. In other words, the use of a traditional competition experiment could indicate saturation at a dose 2- to 10-fold lower than actually required for saturation as identified by ECEX. The ECE magnitude is determined by an interaction of multiple variables, with an overall trend towards a larger ECE in the presence of higher antigen density, high binding affinity, and more rapid internalization rates. Simulations were performed for Ab4 varying each of these parameters individually to validate these trends (data not shown).

While the antibody exhibited the largest magnitude tumor %ID/g, the 2-kDa peptide exhibited lower background and a higher tumor to background ratio, with background defined

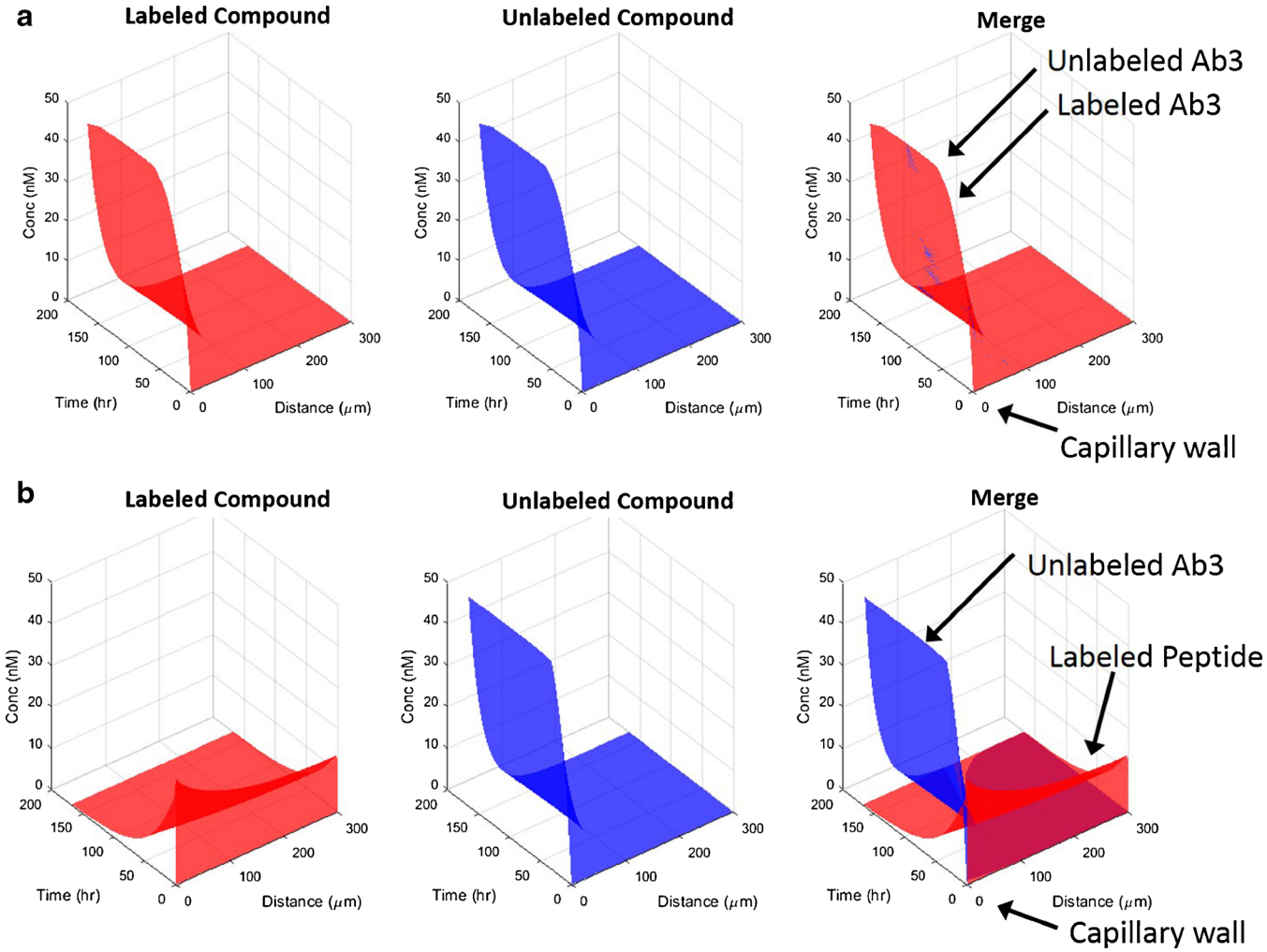

Fig. 5 Nanomolar concentration of labeled construct, unlabeled antibody, and merged plot (from *left* to *right*, respectively) for simulated **a** traditional competition experiment and **b** enhanced competition experiment. Concentration plotted as a function of time and distance from the capillary wall (0 = adjacent to capillary). Labeled 10-μg Ab3 (**a***red*) or labeled 1-μg 2 kDa peptide (**b***red*) co-injected with unlabeled 10-μg Ab3 (*blue*) in a mouse. The human dose would be approximately 3000-fold higher. Vascularity parameter R = 300 μm. Concentration at a distance from the capillary wall is higher for the labeled small construct, as expected (compare *arrows* in (**a**) and (**b**).

as %ID/g present in an antigen-negative tumor (Fig. 6b, d; Supplementary Figs. S3b and S3d). A higher affinity peptide may improve the tumor %ID/g magnitude, especially for lower antigen density levels.

Discussion

A variety of biophysical properties of tumors and antibodies work against homogeneous penetration [1]. Tumors have elevated interstitial pressure which collapses lymphatic vessels and results in transport mediated by diffusion only. This is secondary to disorganized, tortuous blood vessels with high permeability, including leakiness for proteins, as well as compromised lymphatic drainage. These factors lead to high oncotic pressure, drawing in more fluid and raising the interstitial pressure. Interstitial pressure is higher for larger tumors [29], meaning that small tumors in preclinical murine models may not fully reflect the effect of high interstitial pressure observed in the clinic.

Based on the high interstitial pressure, antibody transport is mediated by diffusion only with little to no convective transport. In addition, the tumor extracellular matrix has high content of extracellular matrix proteins such as collagen, which slows diffusion [1]. To fully penetrate, the antibody molecules must diffuse halfway to the nearest blood vessel. While this is likely possible for the “average” intervessel distance, intervessel distances in tumors are highly variable within individual tumors [14]. The time to diffuse varies as the square of the distance: diffusing twice as far takes four times as long.

Antibodies diffuse more slowly than small molecule drugs and nutrients because they have a larger molecular

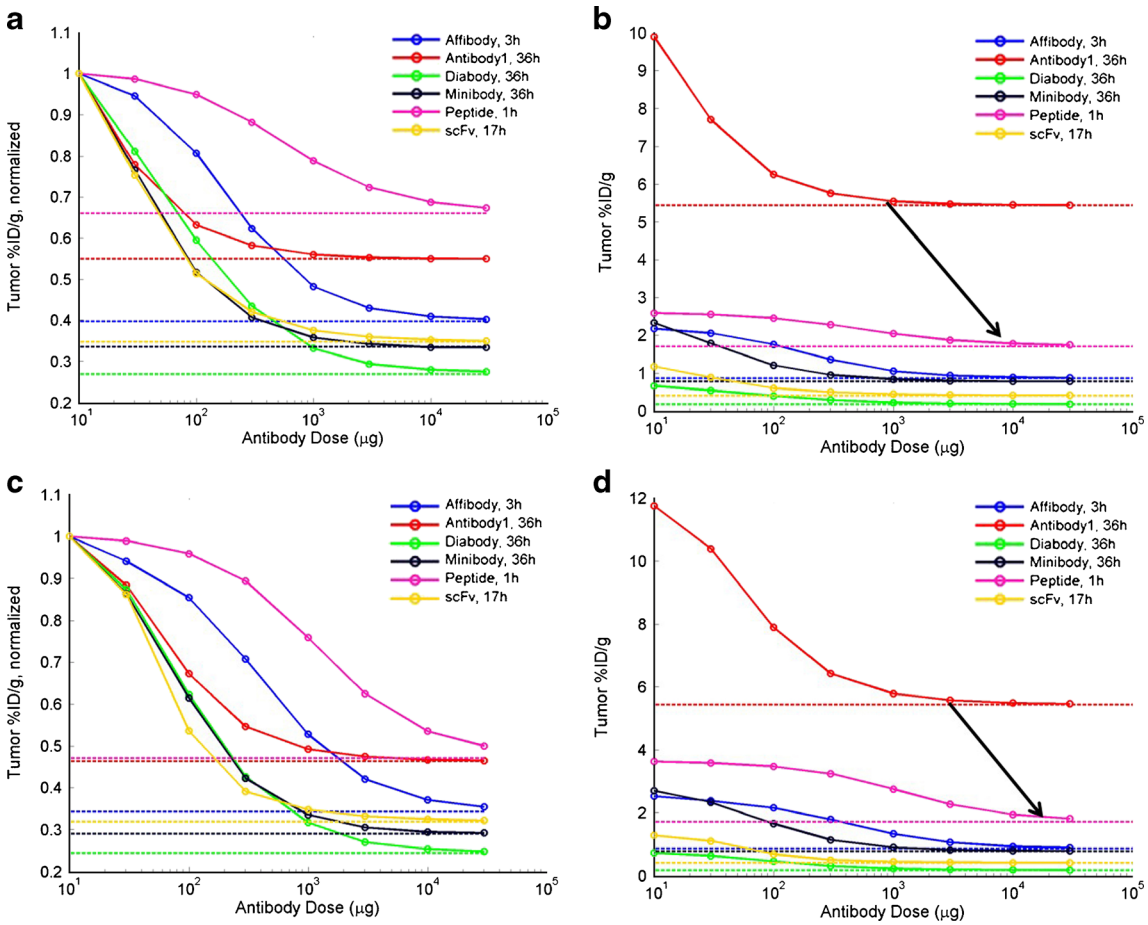

Fig. 6 Normalized (**a**, **c**) and non-normalized (**b**, **d**) tumor %ID/g for radiolabeled construct and increasing unlabeled antibody (**a**, **b** Ab1; **c**, **d** Ab3) dose for simulated enhanced competition experiment. Normalization is to the value in the absence of competing unlabeled antibody. Distribution of intervessel distances is as informed from *(14)*, 1 μg ^{111}In-labeled construct for a 25-g mouse, equivalent to 2.8 mg for an average 70 kg human. The ECE is manifest for the peptide, which requires a higher unlabeled antibody dose to be fully displaced compared with the dose of unlabeled antibody required to displace labeled antibody (*arrows* in (**b**) and (**d**)). *Dotted lines* indicate uptake in an antigen negative tumor with equivalent intervessel distance distribution.

radius [1]. In addition, they carry surface charges and migration can be slowed by non-specific electrostatic interactions with charged elements of the stroma. Moreover, binding to their target as well as internalization can restrict their progress into the tumor. This phenomenon has been termed the "binding site barrier" [30]. Mathematical modeling indicates that antibodies should bind tightly enough to allow cell kill but no tighter, as excessively tight binding may compromise their mobility and penetration [1, 31]. Even in small murine tumors, inhomogeneous penetration has been experimentally demonstrated, and it appears to be a particular concern when affinity for the target is high [32].

At very long distances from blood vessels, small molecule nutrients and oxygen may not diffuse to the location either, and these zones will be necrotic. But in between the limit of therapy diffusion and the more distant limit of small molecule and oxygen diffusion, there may be zones containing living tumor cells that escape therapy. Limited penetration of tumors may be modulated to a degree by co-administration of peptides such as IRGD, a strategy which may be of importance for antibody-drug conjugates which must be delivered at low dose due to inherent toxicity; however, penetration of tumors at low antibody dosage is still quite limited, even in murine tumors with co-administration of IRGD [33].

Penetration and receptor occupancy are functions of mass dose, and this implies a need to optimize dosing for antibody drugs [2]. While methods exist for determining optimal dose for antibody therapy, each has limitations. Given inhomogeneous penetration, it cannot be assumed that pharmacokinetic blood levels reflect concentrations within tumors, or even that the tumor itself is "well mixed," with a single uniform concentration. Antibodies are highly specific and often relatively well tolerated, such that it is not possible to define a "maximum tolerated dose." Pharmacodynamic studies of post-therapy tumor tissues may perhaps allow

dose optimization. However, it is difficult to obtain post-therapy tissues in clinical practice. Moreover, the degree of pharmacodynamic effect corresponding to maximal efficacy is often unknown. Finally, pharmacodynamic assays of tumor tissue will be subject to sampling error in the face of spatial inhomogeneity.

Here, we simulate an enhanced competition experiment, a competition assay in which a labeled small moiety is used to assess receptor occupancy of a larger full-length antibody. The data from these simulations support the hypothesized ECE. While the advantages of low molecular weight constructs (e.g., peptides, affibodies, and other scaffolds <25 kDa) in penetrating into solid tumors was previously known, the current simulations detail the consequences of this fact in the context of a competitive binding experiment for dose determination. Importantly, a higher dose of unlabeled intact antibody was required to block small construct binding to target receptors, which suggests that the ECEX approach may provide a more accurate assessment of the dose required for complete receptor coverage at all locations within the tumor. The implication is that current antibody dose determination paradigms could lead to incomplete target binding and therefore tumor escape at less accessible intratumoral locations. The ECE is seen at sites where the intervessel distance exceeds the median distance traveled by the unlabeled antibody.

The dose of naked antibody required to optimally treat solid tumors is complex and dependent on a range of factors including receptor expression levels, antibody mechanism, and toxicity from antibody treatment [34]. In the absence of dose-limiting toxicity (which is often the case for naked antibodies, as compared with antibody-drug conjugates), the optimal dose for therapeutic effect may be closely linked to the receptor saturating dose. Thus, identification of this dose level is critically important for clinical development [1, 2].

Molecular imaging of antibody uptake in tumors has emerged as a key strategy in defining receptor occupancy in tumors and has been applied in multiple clinical trials [34]. However, imaging of an intact antibody can take over a week for optimal visualization of tumor uptake. ECEX has been proposed as a strategy for quickly identifying receptor occupancy in tumor and for identifying a dose which can penetrate to less accessible sites [2]. The data from this study shows the potential and challenges of this approach.

The penetrance of intact antibody into the center of tumors is restricted by factors including vascularity and blood flow, distance between vessels, interstitial pressure, and necrosis [29–32]. The ECEX approach shows the advantage of using low molecular weight constructs that have the potential for deeper penetrance into tumor. By using intact antibody for competition with low molecular weight constructs, the areas of tumor which cannot be reached by intact antibody, can be identified. This has implications for effective therapy of tumors with intact antibodies and may identify tumors where escape from therapy due to incomplete biodistribution may occur. For areas of tumors with greater than the median intervessel distance, there may be points within the diffusion range of oxygen and small molecule nutrients but not within the diffusion range of full-length monoclonal antibodies given at conventional dosages. Higher dosages may in some instances be required to establish steep concentration gradients to enable diffusion of full-length monoclonal antibodies beyond their usual range.

The parameters used for these simulations were based on published literature of antibody: receptor binding interactions that are typically observed for antibodies that have shown efficacy in the clinic (e.g., trastuzumab and cetuximab). Interestingly, a high receptor number on tumor cells, rapid internalization and high binding affinity all contributed to the ECE effect, which is consistent with the known higher and more heterogeneous uptake in tumor of antibodies that have these characteristics [2].

The implementation of an ECEX approach for clinical trials will face challenges, despite the advantages demonstrated in this simulation study. The small construct must be shown to bind to the same epitope as the antibody so that they can mutually displace each other. In these simulations, we assumed the small construct to have the same affinity as the full-length antibody. It may be challenging to engineer smaller constructs with low nanomolar affinities due to conformational requirements. A relatively large mass dose of unlabeled antibody (on the order of 1–10 g in the clinic, see Fig. 6; Supplementary Fig. S3) will be required to saturate binding sites in the tumor based on these results. This could pose challenges in terms of both cost and protein load. In addition, although relatively high tumor to background ratios will be achievable with low molecular weight constructs *in vivo*, the difference in tumor uptake between construct alone, uptake with a sub-saturating dose of intact antibody, and uptake following blocking with a saturating dose of intact antibody may be challenging to detect in smaller tumors as the projected tumor %ID/g is lower with small constructs compared with intact antibodies (Fig. 6b, d). The benefit of the ECEX requires that we be able to see residual signal present when a dose of unlabeled intact antibody is given that would have appeared to be saturating in a traditional competition experiment but is actually sub-saturating in the ECEX. Radiolabeling with PET tracers (as opposed to SPECT) would provide improved lesion detection and quantitation for this approach in clinical studies [34, 35]. A paired-agent imaging approach [36], with co-administration of non-specific and specific labeled constructs, with dual-isotope SPECT or sequential imaging PET could be used to improve assessment of receptor occupancy with ECEX. Contrast-enhanced CT or MR could be considered to estimate lesion vascular density to support assessment of receptor occupancy with ECEX.

In addition to mass dose, penetration and receptor occupancy are functions of time post-administration. One consideration that was not explored here is a delay between cold antibody and radiolabeled imaging agent administration. Because smaller constructs exhibit faster tissue penetration and have faster clearance, co-administration with unlabeled antibody may result in higher tumor signal than

would be measured if there was a time delay to allow for more antibody penetration into the tumor.

The results presented here have limitations and caveats of a theoretical study. In particular, the isolated Krogh cylinder representation of the tumor does not capture diffusion of molecules from areas of high vascular density (e.g., small Krogh cylinder radii) to areas of low vascular density (large Krogh radii). The simulated results are consistent with published literature on the *in vivo* properties of low molecular weight constructs and penetrance into solid tumors [15]. The simulation utilizes the Krogh cylinder model [11], and the application to ECEX follows similar principles to those employed in evaluating the impact of antibody construct size on tumor uptake [15]. Further assessment of the validity of this approach will be best addressed with *in vivo* experimentation and ultimately in human trials.

Conclusions

Regarding the questions posed in the "Introduction," this simulation study has demonstrated that (1) The ECEX can be simulated mathematically. (2) Radiolabeled low molecular weight constructs, due to their more optimal tumor penetration, reveal the need for higher doses of intact antibody for complete receptor occupancy. Incomplete receptor occupancy at less accessible sites may lead to tumor escape from therapy. (3) Increased receptor density, fast internalization, and high binding affinity contribute to a larger ECE effect. (4) Low molecular weight constructs (<25 kDa), that have the potential for deeper penetrance into tumor, are most optimal for ECEX. (5) The difference in imaging signal between sub-saturating and saturating antibody doses in the presence of labeled small constructs is small and may be challenging to detect *in vivo* using current clinical imaging technology. These results will inform the design of future *in vivo* studies aimed at determining the optimal dose of antibody for oncology therapeutic trials.

Compliance with Ethical Standards

Conflict of Interest

KDO and JH are full-time employees and stockholders of inviCRO. MS is a former employee and owns stock in inviCRO. JG is a full-time employee of Daiichi Sankyo, Inc. and owns stock in Daiichi Sankyo. MK is a full-time employee of Daiichi Sankyo. MM is a former employee and owns stock in Daiichi Sankyo. GPA and AMW are consultants to Daiichi Sankyo. GPA is a full-time employee of Viventia Bio. AMS has received funding/research support from Daiichi Sankyo. RAB is a former employee of Daiichi Sankyo and owns stock in Johnson and Johnson. This work was funded in part by Daiichi Sankyo, Inc.

References

1. Beckman RA, Weiner LM, Davis HM (2007) Antibody constructs in cancer therapy: protein engineering strategies to improve exposure in solid tumors. Cancer 109:170–179
2. Beckman RA, von Roemeling R, Scott AM (2011) Monoclonal antibody dose determination and biodistribution into solid tumors. Ther Deliv 2:333–344
3. Thurber GM, Wittrup KD (2012) A mechanistic compartmental model for total antibody uptake in tumors. J Theor Biol 314:57–68
4. Kurai J, Chikumi H, Hashimoto K et al (2007) Antibody-dependent cellular cytotoxicity mediated by cetuximab against lung cancer cell lines. Clin Cancer Res 13:1552–1561
5. Meerten TV, van Rijn RS, Hol S et al (2006) Complement-induced cell death by rituximab depends on CD20 expression level and acts complementary to antibody-dependent cellular cytotoxicity. Clin Cancer Res 12:4027–4035
6. Bellosillo B, Villamor N, Lopez-Guillermo A et al (2001) Complement-mediated cell death induced by rituximab in B-cell lymphoproliferative disorders is mediated in vitro by a caspase-independent mechanism involving the generation of reactive oxygen species. Blood 98:2771–2777
7. Hendriks BS, Opresko LK, Wiley HS et al (2003) Quantitative analysis of HER2-mediated effects on HER2 and epidermal growth factor receptor endocytosis: distribution of homo- and heterodimers depends on relative her2 levels. J Biol Chem 278:23343–23351
8. Rudnick SI, Lou J, Shaller CC et al (2011) Influence of affinity and antigen internalization on the uptake and penetration of anti-HER2 antibodies in solid tumors. Cancer Res 71:2250–2259
9. Herter S, Herting F, Mundigl O et al (2013) Preclinical activity of the type II CD20 antibody GA101 (obinutuzumab) compared with rituximab and ofatumumab in vitro and in xenograft models. Mol Cancer Ther 12:2031–2042
10. Eiblmaier M, Meyer LA, Watson MA et al (2008) Correlating EGFR expression with receptor-binding properties and internalization of 64CU-DOTA-cetuximab in 5 cervical cancer cell lines. J Nucl Med 49:1472–1479
11. Krogh A (1919) The supply of oxygen to the tissues and the regulation of the capillary circulation. J Physiol 52(6):457–474
12. Thurber GM, Zajic SC, Wittrup KD (2007) Theoretic criteria for antibody penetration into solid tumors and micrometastases. J Nucl Med 48(6):995–999
13. Baxter LT, Jain RK (1996) Pharmacokinetic analysis of the microdistribution of enzyme-conjugated antibodies and prodrugs: comparison with experimental data. Br J Cancer 73(4):447–456
14. Lauk S, Zietman A, Skates S et al (1989) Comparative morphometric study of tumor vasculature in human squamous cell carcinomas and their xenotransplants in athymic nude mice. Cancer Res 49:4557–4561
15. Schmidt MM, Wittrup KD (2009) A modeling analysis of the effects of molecular size and binding affinity on tumor targeting. Mol Cancer Ther 8(10):2861–2871
16. Orcutt KD, Nasr KA, Whitehead DG et al (2011) Biodistribution and clearance of small molecule hapten chelates for pretargeted radioimmunotherapy. Mol Imaging Biol 13(2):215–221
17. Orlova A, Magnusson M, Eriksson TL et al (2006) Tumor imaging using a picomolar affinity HER2 binding affibody molecule. Cancer Res 66:4339–4348
18. Tolmachev V, Nilsson FY, Widstrom C et al (2006) 111In-benzyl-DTPA-ZHER2:342, an affibody-based conjugate for in vivo imaging of HER2 expression in malignant tumors. J Nucl Med 47:846–853
19. Williams LE, Wu AM, Yazaki PJ et al (2001) Numerical selection of optimal tumor imaging agents with application to engineered antibodies. Cancer Biother Radiopharm 16:25–35
20. Willuda J, Kubetzko S, Waibel R et al (2001) Tumor targeting of mono-, di-, and tetravalent anti-p185(HER-2) miniantibodies multimerized by self-associating peptides. J Biol Chem 276:14385–14392
21. Kubetzko S, Balic E, WWaibel R et al (2006) PEGylation and multimerization of the anti-p185HER-2 single chain Fv fragment 4D5: effects on tumor targeting. J Biol Chem 281:35186–35201
22. Tai M (1995) Targeting c-erbB-2 expressing tumors using single-chain Fv monomers and dimers. Cancer Res 55(23 Suppl):5983s–5989s
23. Nielsen UB, Adams GP, Weiner LM et al (2000) Targeting of bivalent anti-ErbB2 diabody antibody fragments to tumor cells is independent of the intrinsic antibody affinity. Cancer Res 60:6434–6440
24. Olafsen T, Kenanova VE, Sundaresan G et al (2005) Optimizing radiolabeled engineered anti-p185HER2 antibody fragments for in vivo imaging. Cancer Res 65:5907–5916
25. Olafsen T, Tan GJ, Cheung CW et al (2004) Characterization of engineered anti-p185HER-2 (scFv-CH3)2 antibody fragments (minibodies) for tumor targeting. Protein Eng Des Sel 17:315–323
26. Tsai SW, Sun Y, Williams LE et al (2000) Biodistribution and radioimmunotherapy of human breast cancer xenografts with

radiometal-labeled DOTA conjugated anti-HER2/neu antibody 4D5. Biocong Chem 11:327–334
27. De Santes K, Slamon D, Anderson SK et al (1992) Radiolabeled antibody targeting of the HER-2/neu oncoprotein. Cancer Res 52:1916–1923
28. Pedley RB, Boden JA, Boden R et al (1994) The potential for enhanced tumour localization by poly(ethylene glycol) modification of anti-CEA antibody. Br J Cancer 70(6):1126–1130
29. Gutmann R, Leunig M, Feyh J et al (1995) Interstitial hypertension in head and neck tumors in patients: correlation with tumor size. Cancer Res 52:1993–1995
30. Graff CP, Wittrup KD (2003) Theoretical analysis of antibody targeting of tumor spheroids: importance of dosage for penetration, and affinity for retention. Cancer Res 63:1288–1296
31. Adams GP, Schier R, McCall AM et al (2001) High affinity restricts the localization and tumor penetration of single chain Fv antibody molecules. Cancer Res 61:4750–4755
32. Hussain S, Rodriguez-Fernandez M, Bruan GM et al (2014) Quantity and accessibility for specific targeting of receptors in tumors. Sci Rep 4:5232
33. Fujimori K, Covell DG, Fletcher JE et al (1990) A modeling analysis of monoclonal antibody percolation through tumors: a binding site barrier. J Nucl Med 31:1191–1198
34. Scott AM, Wolchok JD, Old LJ (2012) Antibody therapy of cancer. Nat Rev Cancer 12(4):278–287
35. Knowles SM, Wu AM (2012) Advances in immune-positron emission tomography: antibodies for molecular imaging in oncology. J Clin Oncol 30(31):3884–3892
36. Tichauer KM, Wang Y, Pogue BW et al (2015) Quantitative in vivo cell-surface receptor imaging in oncology: kinetic modeling and paired-agent principles from nuclear medicine and optical imaging. Phys Med Biol 60(14):R239–R269